

# The impact of tau hyperphosphorylation at Ser<sup>262</sup> on memory and learning after global brain ischaemia in a rat model of reversible cardiac arrest



Shohreh Majd<sup>a,\*</sup>, John H.T. Power<sup>b</sup>, Simon A. Koblar<sup>c</sup>, Hugh J.M. Grantham<sup>a</sup>

<sup>a</sup> *Neuronal Injury and Repair Laboratory, Centre for Neuroscience, School of Medicine, Flinders University, Adelaide, Australia*

<sup>b</sup> *Department of Human Physiology, School of Medicine, Flinders University, Adelaide, Australia*

<sup>c</sup> *School of Medicine, The Queen Elizabeth Hospital (TQEH) Campus, University of Adelaide, Australia*

## ARTICLE INFO

### Article history:

Received 19 October 2016

Received in revised form

12 December 2016

Accepted 21 December 2016

### Keywords:

Tau phosphorylation

Glycogen synthase Kinase-3 $\beta$

Protein phosphatase 2A

Liver kinase B1

Adenosine monophosphate kinase protein kinase

Ischaemia/reperfusion

## ABSTRACT

An increase in phosphorylated tau (p-tau) is associated with Alzheimer's disease (AD), and brain hypoxia. Investigation of the association of residue-specific tau hyperphosphorylation and changes in cognition, leads to greater understanding of its potential role in the pathology of memory impairment. The aims of this study are to investigate the involvement of the main metabolic kinases, Liver Kinase B1 (LKB1) and Adenosine Monophosphate Kinase Protein Kinase (AMPK), in tau phosphorylation-derived memory impairment, and to study the potential contribution of the other tau kinases and phosphatases including Glycogen Synthase Kinase (GSK-3 $\beta$ ), Protein kinase A (PKA) and Protein Phosphatase 2A (PP2A). Spatial memory and learning were tested in a rat global brain ischemic model of reversible cardiac arrest (CA). The phosphorylation levels of LKB1, AMPK, GSK-3 $\beta$ , PP2A, PKA and tau-specific phosphorylation were assessed in rats, subjected to ischaemia/reperfusion and in clinically diagnosed AD and normal human brains. LKB1 and AMPK phosphorylation increased 4 weeks after CA as did AMPK related p-tau (Ser<sup>262</sup>). The animals showed unchanged levels of GSK-3 $\beta$  specific p-tau (Ser<sup>202</sup>/Thr<sup>205</sup>), phospho-PP2A (Tyr<sup>307</sup>), total GSK-3 $\beta$ , PP2A, phospho-cAMP response element-binding protein (CREB) which is an indicator of PKA activity, and no memory deficits. AD brains had hyperphosphorylated tau in all the residues of Ser<sup>262</sup>, Ser<sup>202</sup> and Thr<sup>205</sup>, with increased phosphorylation of both AMPK (Thr<sup>172</sup>) and GSK-3 $\beta$  (Ser<sup>9</sup>), and reduced PP2A levels. Our data suggests a crucial role for a combined activation of tau kinases and phosphatases in adversely affecting memory and that hyperphosphorylation of tau in more than one specific site may be required to create memory deficits.

© 2016 The Authors. Published by Elsevier Ltd on behalf of International Brain Research Organization.

This is an open access article under the CC BY-NC-ND license

(<http://creativecommons.org/licenses/by-nc-nd/4.0/>).

## 1. Introduction

Many studies have reported cognitive behaviour and memory impairments as the long-term outcomes of brain hypoxia (Pohjasvaara et al., 1998; Madureira et al., 2001; Mateen et al., 2011; Sun et al., 2014). The relationship of Alzheimer's disease (AD) type dementia and a history of head injury has been noted (Plassman et al., 2000) and a suggested explanation links hypoxia and over-expression of phosphorylated tau (p-tau), seen in head injury and

AD demonstrated in an animal model of cerebral hypoxia (Castro-Alvarez et al., 2011; Iliff et al., 2014; Zhang et al., 2014; Asai et al., 2015).

Tau hyperphosphorylation is one of the suggested theories explaining AD pathophysiology (Stoothoff and Johnson, 2005; Hanger et al., 2009). Previous reports demonstrated that hypoxic insults to cortical neurons triggered pathological cascades such as tau hyperphosphorylation (Chen et al., 2003). Other evidence from animal studies indicated that hypoxia and ischaemia facilitated the generation of AD pathological hallmarks in rats via many mechanisms, resulting in hyperphosphorylated tau and beta amyloid (Stephenson et al., 1992; Xie et al., 2005; Castro-Alvarez et al., 2011; Zhang et al., 2014).

A balance of activity between glycogen synthase kinase-3 $\beta$  (GSK-3 $\beta$ ) and protein phosphatase 2A (PP2A), as the main tau kinase and phosphatase has been reported as the core contributor

\* Corresponding author. Neuronal Injury and Repair Laboratory, Flinders Medical Centre, Level 6, Rm 6E404 Bedford Park, SA 5042, Australia.

E-mail addresses: [shohreh.majd@flinders.edu.au](mailto:shohreh.majd@flinders.edu.au) (S. Majd), [john.power@flinders.edu.au](mailto:john.power@flinders.edu.au) (J.H.T. Power), [simon.koblar@adelaide.edu.au](mailto:simon.koblar@adelaide.edu.au) (S.A. Koblar), [hugh.grantham@flinders.edu.au](mailto:hugh.grantham@flinders.edu.au) (H.J.M. Grantham).

in defining tau phosphorylation/dephosphorylation status (Eldar-Finkelman, 2002; Liu et al., 2005). This theory is supported by several reports from post-mortem studies of brains from clinically diagnosed AD patients which demonstrated tangle-bearing neurons associated with a high level of GSK-3 $\beta$  (Lovell et al., 2004; Hernandez et al., 2013) and a reduction of activity of PP2A through increasing its phosphorylation at Tyr<sup>307</sup>. Phosphorylation of PP2A at Tyr<sup>307</sup> has also been reported in tangle-bearing neurons in patients with AD (Gong et al., 1995; Sontag et al., 2004). These findings suggest that GSK-3 $\beta$  and PP2A may be involved in the promotion of tau aggregation in AD (Hanger et al., 2007; Hanger and Noble, 2011), however more recent reports have shown that some hyperphosphorylated residues of tau in AD brains, are insensitive to the action of GSK-3 $\beta$  and PP2A (Guerra-Araiza et al., 2007; Hanger et al., 2007; Hanger and Noble, 2011), raising the question of the importance of the other kinases as well as the site-related phosphorylation of tau in generating AD pathology.

It appears that tau phosphorylation is dependent on more than just GSK-3 $\beta$  and PP2A. Tau can be phosphorylated at over 40 sites of Ser/Thr residues (Hanger et al., 2007), by a series of other kinases including Protein kinase A (PKA) (Liu et al., 2006), Cyclin-dependent Kinase 5 (cdk5) and the Adenosine Monophosphate Kinase Protein Kinase (AMPK) family (Johnson and Stoothoff, 2004; Chatterjee et al., 2009; Castro-Alvarez et al., 2011; Thornton et al., 2011; Yoshida and Goedert, 2012), all these kinases could be activated by neuronal stress.

A link exists between tau phosphorylation and neuronal stability in response to stressful conditions such as ischaemia (Dewar and Dawson, 1995; van der Harg et al., 2014). An early response to ischaemia/hypoxia is activation of the master regulator of cellular metabolism, Liver Kinase B1 (LKB1) and subsequently AMPK-related kinases, which also possess tau kinase activity. AMPK kinases mainly phosphorylate tau at Ser<sup>262</sup>, a GSK-3 $\beta$ -insensitive site that is phosphorylated early in the process of AD (Augustinack et al., 2002; Guerra-Araiza et al., 2007; Mairet-Coello et al., 2013; Domise et al., 2016). Phosphorylation of tau at Ser<sup>262</sup> is reported as a critical component of tau-induced toxicity (Iijima et al., 2010). The correlation between the AMPK modulatory function on metabolism in response to hypoxia/anoxia (Hardie, 2011) and its tau kinase activity suggests a metabolic based hypothesis for the pathophysiology of AD. However to what extent the phosphorylation of Ser<sup>262</sup>, an AMPK kinases-sensitive site of tau without the involvement of the other major kinases and phosphatases of tau could affect the memory function requires investigation.

We previously demonstrated in a reversible rat model of cardiac arrest (Majd et al., 2016), that brain ischaemia significantly attenuated p-tau within the first few minutes. In this study, we investigated AMPK-sensitive tau phosphorylation of Ser<sup>262</sup> due to changes in LKB1/AMPK activity in response to alterations in brain oxygenation. We showed that recovery from global brain ischaemia is associated with hyperactivity of AMPK and tau hyperphosphorylation at Ser<sup>262</sup>. Because in our model the observed hyperphosphorylation at Ser<sup>262</sup> alone was not associated with observed changes in memory and learning, we suggest that this residue-specific hyperphosphorylation in the absence of changes in the levels of other tau kinases and phosphatases such as PKA, GSK-3 $\beta$  and PP2A, was not enough to create an impact on memory and learning in rats. Combining the results of our animal experiments, with the findings from our human studies of Alzheimer's patients, we suggest the involvement of at least three enzymes; AMPK, GSK-3 $\beta$  and PP2A in generating the neuropathological forms of tau in the hippocampus and mid-frontal gyrus (MFG) seen in AD.

## 2. Experimental procedures

### 2.1. Animal experiments

The animal study was approved by the Animal Ethics Committee of Flinders University and was completed in accordance with the South Australian Prevention of Cruelty to Animals Act 1985 following the Australian Code of Practice for the Care and Use of Animals for Scientific Purposes, 2004.

### 2.2. Animal preparation

Adult Sprague-Dawley rats (2 months, 250–350 g, female) from Laboratory Animal Services (Adelaide University) were used, in 4 experimental groups (n = 6 in each). The experimental time line is illustrated in Fig. 1. Reversible cardiac arrest (CA) was generated under general anaesthesia, using our previously described model (Majd SP et al., 2016). In this model electrocardiogram leads are attached to the chest, allowed constant recording of cardiac electrical activity and defibrillation via a defibrillator/monitor (Philips HeartStart MRX, Philips Healthcare INC, USA). Oxygen saturation (SpO<sub>2</sub>) and pulse rate were continuously monitored via a Pulse-oximeter. Ventilation with supplemental oxygen was performed via endotracheal intubation using a volume-controlled small animal ventilator (New England Medical Instruments Inc, Medway, Massachusetts, USA). The body temperature was checked by rectal probe, and was maintained with a heating lamp.

CA was achieved using two phases of transoesophageal alternating current (50Hz 24V followed by 50Hz 18V) via a pacing catheter with two end ring electrodes and a 0.5 cm gap inserted in the oesophagus to a depth of 6–6.5 cm. Ventilation was stopped during CA. A post CA rhythm of ventricular fibrillation was defibrillated using 8 J. Effective circulation was confirmed by a pulse oximeter reading, a SpO<sub>2</sub> of 85–95% or greater was maintained. Two min of CA was followed by post resuscitation perfusion (60 min: short-term recovery; 4 weeks: long-term recovery).

To obtain brain samples, the brains were perfused with cold Phosphate Buffered Saline, half of the specimen was frozen in liquid nitrogen after isolation and kept in a –80 °C freezer and half was fixed in 10% paraformaldehyde. Five  $\mu$ m sections of the brain containing the hippocampus and cortex were placed on Poly-d-Lysine coated slides, deparaffinized in xylene, and dehydrated in ethanol.

### 2.3. Novel object recognition (NOR)

To assess learning and memory, the animal's response to a familiar object compared to its response to a novel object was tested (n = 6 in this group), before CA and after 4 weeks recovery. The animals were given a 30 min habituation period prior to starting the test, to gain familiarity with the arena. In the acquisition stage of the test the rats were allowed to explore two identical objects in an experimental chamber for 10 min, the exploration time around each object was measured. Memory retention was assessed when one of the identical objects was replaced with a novel one during a retention trial (10 min) either after an inter-trial interval of 1 h of (representing the short-term memory retention) or after 24 h (representing long-term memory retention). The time spent exploring the objects was analysed as previously described (Bevins and Besheer, 2006) as follows: (Time around novel – Time around familiar object)/(Time around novel object + Time around familiar object) and was analysed using ANY-maze software (Stoelting Co, Wood Dale, IL, USA).

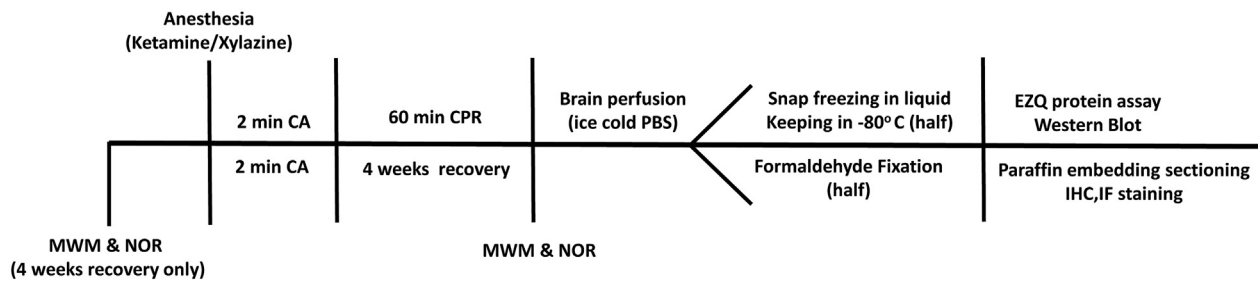


**Fig. 1.** Timeline of the animal study: behavioural test of Morris Water Maze (MWM) and Novel Object Recognition (NOR) for memory and learning assessment were performed before and 4 weeks after cardiac arrest (CA). Western blot and immuno-staining were used for protein assessment and protein visualization.

#### 2.4. Morris Water Maze (MWM)

Spatial memory was assessed using a Morris Water Maze (MWM) as described previously (Tonkiss et al., 2003). Each rat was subjected to two complete series of MWM assessments, before CA and after CA ( $n = 6$  in this group). Individual variations in learning and memory ability between animals were accounted for by using each rat as its own control and comparing memory after CA with memory before CA in the same animal. A circular pool (150 cm in diameter with 60 cm high walls) was divided into 4 equal quadrants, filled with water (to a depth of 40 cm) that was made opaque with skim milk (99% fat free). The water temperature was adjusted to  $25^\circ (\pm 0.5)$  C. Coloured shapes were placed on the wall of the room, as visual cues. The rat's movement was recorded using a camera above the pool and a computer running the ANY-maze software (Stoeling Co, Wood Dale, IL, USA). Before starting the trial phase of the test, each rat was allowed an adaptation period of 30 min to the room environment. Each test contained three phases: visible-platform training, probe test and hidden-platform training.

##### 2.4.1. Training phase with visible-platform

The visible platform (10 cm in diameter), was placed in one quadrant of the pool (North West: NW, Fig. 5), 1.5 cm above the water and easily visible to the rat. Each rat was given 1 min on the platform before undergoing 3 swim training trials.

Each rat was trained to remember the location of the visible platform, by being released from three different quadrants (North-east: NE, South-east: SE and South-west: SW) facing the wall at a distance of 30–45 cm. The rats were given 1 min each in each trial to reach to the platform. If the rat was not able to find the platform within 1 min, it was guided by the examiner's hand toward the platform and the time was recorded as 1 min. Upon standing on the platform, the animal was allowed to remain there for 15 s. Each rat was subjected to 12 trials over two days (6 trials each day) in total, with a 45 min interval time between each trial, when the rat was dried and placed in a heated cage.

For each rat, the platform location remained unchanged while the starting position was changed randomly on each trial, making sure that each starting location was repeated twice in each day containing 6 trials.

##### 2.4.2. Probe test

The probe test was performed on the day three of the test. During each test the platform was removed and the rat was released from four starting points of NW, NE, SW and SE. To assess the establishment of the learning strategy (spending more time in the target quadrant) the rats were given 1 min to swim freely during each of the four trials, and the time spent in each quadrant was calculated.

##### 2.4.3. Training phase with hidden-platform

In the hidden phase of the test, the platform was submerged (1 cm under water). Two sets of 6 trials (12 trials in total) were

performed with a 30–45 s recovery period between each trial and 30–45 min between the first set (6 trials) and the second set of 6 trials. Each rat was given 1 min to find the platform, followed by a 15 s reinforcement time when the rat remained on the platform. If the rat was not able to reach the platform within 1 min, it was guided by the examiner's hand toward the platform and the time were recorded as 1 min. Time to reach the platform (latency) and time spent in the target quadrant was recorded and analysed using a video tracking system (Stoeling Co, Wood Dale, IL, USA).

#### 2.5. Human experiments

Brain tissues from six clinically diagnosed AD (confirmed pathologically postmortem) and three control cases (without confirmed diagnosed neurological pathology postmortem) were obtained from the National Health and Medical Research Council South Australian Brain Bank and analysed using a western blot and antibody technique. Table 1 provides a list of the brain regions examined and the case details.

#### 2.6. Antibodies

Phosphorylated LKB1 mouse-monoclonal (Ser<sup>431</sup>; sc-271924), LKB1 rabbit-polyclonal (H-75; sc-28788), p-tau rabbit-polyclonal (Ser<sup>262</sup>; sc-101813), p-GSK-3 $\beta$  goat-polyclonal (Ser<sup>9</sup>; sc-11757), p-PP2A-C $\alpha$ / $\beta$  mouse-monoclonal (F-8; sc-271903), tau mouse-monoclonal (A-10; sc-390476), GSK-3 $\beta$  rabbit-polyclonal (H-76; sc-9166), p-CREB (Ser<sup>133</sup>; sc-101663) rabbit-polyclonal and PP2A-A $\alpha$  goat-polyclonal antibodies (C-20; sc-6112) were purchased from Santa Cruz. Mouse-monoclonal GFAP and Ser<sup>202</sup>/Thr<sup>205</sup> (AT8) antibodies were obtained from Professor John Power from the Alzheimer's and Parkinson's laboratory (Flinders University). Phosphorylated AMPK rabbit-polyclonal (Thr<sup>172</sup>, #2531) and AMPK rabbit-polyclonal antibodies (#2532) were purchased from Cell Signalling Australia. Mouse NeuN antibody (MAB377) was purchased from Merck Millipore Australia. Secondary antibodies of HRP donkey anti-mouse (715-036-150), anti-rabbit (711-035-

**Table 1**

List of the human cases used for protein assessment via western blot analysis.

Case number	Sex	Age (yr)	Diagnosis	Region	PMI (hrs)
SA0163	F	72	AD	Hippocampus	12
SA0168	F	82	AD	Hippocampus	8
SA0215	F	77	AD	Hippocampus	17
SA0237	M	81	AD	MFG	21
SA0244	M	63	AD	Hippocampus	23
SA0248	M	83	AD	Hippocampus	37
SA0112 (C)	F	86	MLI	MFG	6
SA0214 (C)	M	64	HP	Hippocampus	36
SA0230 (C)	M	86	Other	Hippocampus	22

PMI = post mortem interval; AD = Alzheimer's disease; C = Control; M = male; F = female; MFG = middle frontal gyrus; HP = hypertension; MLI = multiple lacunar infarcts.

152), anti-goat (705-035-003) and goat anti rabbit (111-035-144), Biotinylated donkey anti-rabbit (711-065-152), Alexa Fluor® 488 donkey anti-rabbit, Alexa Fluor® CY3 donkey anti-mouse and Alexa Fluor® CY3 donkey anti-sheep were purchased from Jackson ImmunoResearch (West Grove, USA).

### 2.7. Brain homogenate

Frozen tissue from the hippocampus and mid-frontal gyrus (MFG) of six AD and three control cases (human brains) and the middle 1/3 (0.3–0.35 g) of the frozen specimens (rat brains) containing parietal cortex and hippocampus were homogenized in extraction buffer (50 mM Tris, 5 mM EDTA, 0.1% sodium azide, Pepstatin A (Sigma, P5318, 1 µg/ml), Leupeptin (Sigma, L2884, 1 µg/ml) and phenylmethylsulfonyl fluoride (Sigma, P7626, 100 mM)), centrifuged (1000g/5 min) and the supernatants were analysed.

### 2.8. Protein quantification and western blot analysis

The amount of total protein in each sample was calculated using an EZQ assay following an approved protocol (Bio-Rad, Hercules, CA). To analyse electrophoretic mobility of p-LKB1, LKB1, p-tau, tau, p-GSK-3β, GSK-3β, p-PP2A, PP2A, p-CREB, p-AMPK and AMPK, 30 µg of each sample was loaded in each well of AnykD™ TGX Stain-free gel (Bio-Rad, CA, USA, 569033), with 1 well containing 5 µL Precision Plus Protein™ Dual Color Standards (Bio-rad, Hercules, CA, USA). A current (300 mA) was applied to the gel for 20 min. Samples were blotted using a Bio-Rad Trans-Blot transfer system kit (Bio-Rad, CA, USA). The membranes were blocked for 1 h and were incubated overnight (4 °C) with primary antibodies of p-tau (Ser<sup>262</sup>, 1:250), AT8 (Ser<sup>202</sup>/Thr<sup>205</sup>, 1:1000), p-GSK-3β (1:500), p-PP2A-Cα/β (1:500), tau (1:250), GSK-3β (1:500), PP2A-Aα (1:500), p-LKB1 (1:500), LKB1 (1:500), p-AMPK (1:1000), AMPK (1:1000). Following this the membranes were incubated for 1 h with HRP secondary antibodies (donkey anti-mouse and anti-rabbit, 1:3000; donkey anti-goat, 1:10,000). The blots were developed using an ECL and chemiluminescence signal detection was performed using Fuji LAS4000 imager, quantitated by CareStream imaging software, and were corrected against actin levels.

### 2.9. Immunohistochemistry (IHC) and immunofluorescent (IF)

(DAB)-metal enhanced IHC and IF staining were undertaken using an established process (Power et al., 2015; Majd et al., 2016). Briefly, 5 µm brain sections of parietal cortex and hippocampus of the rats were deparaffinised. After EDTA antigen retrieval, the sections were incubated with hydrogen peroxidase and horse serum blocking, followed by incubating with p-tau (Ser<sup>296</sup>, 1:200), p-AMPK (Thr<sup>172</sup>, 1:200), p-LKB1 (Ser<sup>431</sup>, 1:200), p-GSK-3β (Ser<sup>9</sup>, 1:200), tau (1:200), NeuN (1:200) and GFAP (1:200) antibodies (18 h/4 °C). The sections were subsequently incubated for 1 h with the Biotinylated donkey anti-rabbit, and anti-mouse for IHC (1:1000, Jackson) and Alexa Fluor® 488 donkey anti-rabbit, CY3 donkey anti-mouse, Alexa Fluor® 488 donkey anti-mouse and CY3 donkey anti-sheep (1:100, Jackson) for IF. The staining was visualized using a Brightfield Olympus BX50 and Leica SP5 5-channel laser scanning confocal microscope.

### 2.10. Statistical analysis

All data were analysed using IBM Statistics version of SPSS Software and the results were expressed as the mean ± SD. One-way ANOVA was used to assess the differences between the means of the groups followed by *post hoc* Tukey's. Student independent t-tests were used to assess the differences between two human groups of normal and AD cases. Student Paired t-tests were used to assess

the difference between NOR and MWM tests before and after CA. Significance was defined as \**p* < 0.05.

## 3. Results

### 3.1. Rat model of reversible global brain ischaemia

A rat model of reversible cardiac arrest (CA) was used to investigate the effect of ischaemia and recovery from ischaemia, on the main metabolic axis of LKB1/AMPK. Analysing a series of brain tissue samples, obtained from animals subjected to different periods of ischaemia/reperfusion showed the following results:

#### 3.1.1. Effect of ischaemia on LKB1/AMPK axis activation

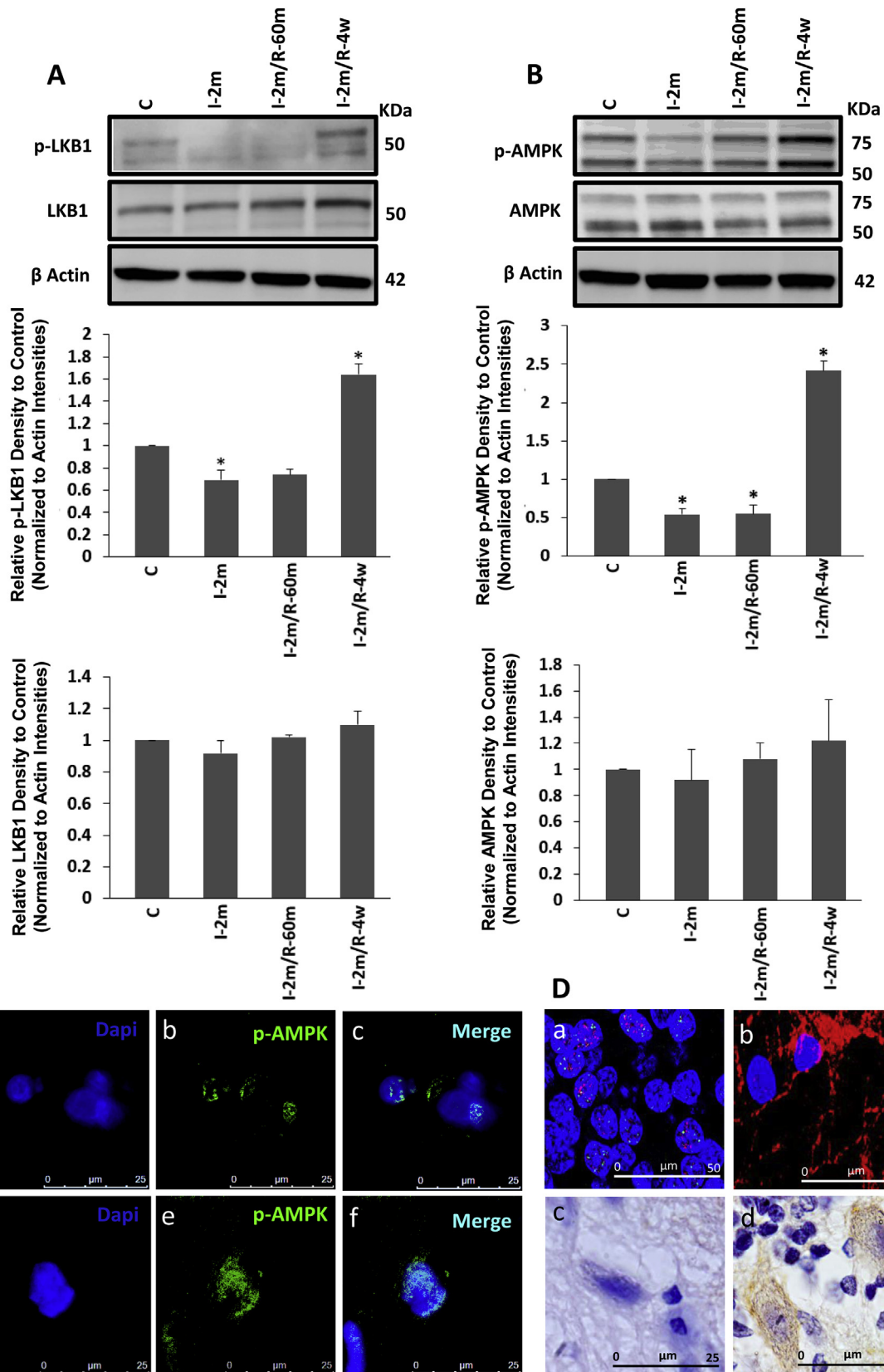
The levels of LKB1 and AMPK phosphorylation were evaluated at different time points to assess the effect of global brain ischaemia/reperfusion on this main cellular metabolic axis. Following an initial reduction of p-LKB1 (active form) during 2 min of ischaemia (One Way ANOVA,  $F_{3,20} = 77.16$ , \**p* < 0.05), p-LKB1 showed a significant increase after 4 weeks of recovery following CA (One Way ANOVA,  $F_{3,20} = 77.16$ ,  $P = 0.000538$ , \**p* < 0.01) (Fig. 2A). The western blot result was confirmed by DAB staining, showing an enhanced immunostaining of p-LKB1 in the brains of the rats after 4 weeks recovery (2D. d) compared to the control group (2D. c). Western blot results showed an enhanced AMPK phosphorylation level after the same period of 4 weeks recovery following 2 min of CA (One Way ANOVA,  $F_{3,20} = 224.4$ , \**p* < 0.01) (Fig. 2B). These findings were supported by the immunofluorescent results, showing higher accumulation of p-AMPK (green) in the long-term recovery (Fig. 2C d, e, f) compared with the control group (Fig. 2C a, b, c), with a greater distribution of p-AMPK within the neurons (nuclear staining with NeuN in red (2D. a)) compared with glial cells (cytoplasmic glial fibrillary acidic protein (GFAP) staining in red (2D. b)). This represents an increase in p-LKB1 and p-AMPK in the 4 weeks after ischaemia recovery groups as the total amount of AMPK and the level of β-actin remained the same across all lanes (Fig. 2A and B).

#### 3.1.2. Effect of ischaemia on tau phosphorylation at AMPK-sensitive epitope (Ser<sup>262</sup>), and GSK-3β-sensitive epitope (Ser<sup>202</sup>/Thr<sup>205</sup> (AT8))

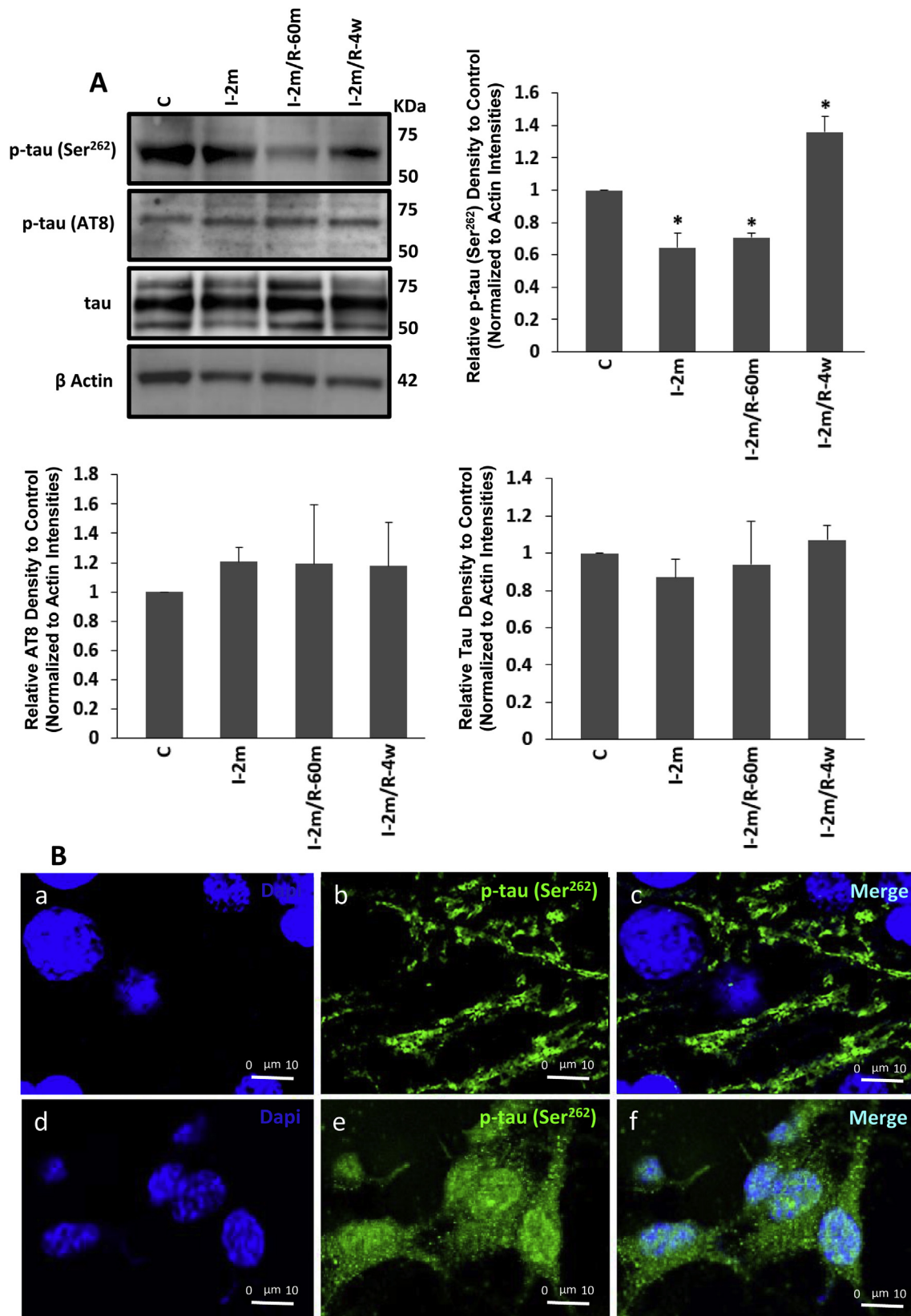
To determine the involvement of AMPK and GSK-3β in tau phosphorylation during ischaemia and reperfusion, the homogenates containing parietal cortical and hippocampal tissues were used for Western blot analysis to assess the levels of p-tau (Ser<sup>262</sup>, Ser<sup>202</sup>/Thr<sup>205</sup>) and total tau in 2 min ischaemia and 2 min ischaemia followed by 1 h and 4 weeks recovery vs control (anesthesia only). The actin loading was assessed across the different groups. An initial reduction in p-tau at Ser<sup>262</sup>, (AMPK specific residue) was followed by a significant increase after 4 weeks (One Way ANOVA,  $F_{4,20} = 96.62$ , \**p* < 0.01). AMPK independent but GSK-3β dependent p-tau (Ser<sup>202</sup>/Thr<sup>205</sup>), remained unchanged (Fig. 3A). To examine the possibility of underlying changes in total tau being responsible for the observed results the levels of total tau in all groups were tested. The results showed that 2 min ischaemia did not affect the total tau while phosphorylation at its AMPK-sensitive residue was affected (Fig. 3A). The impact of ischaemia on p-tau at Ser<sup>262</sup> was observed in the IF staining after 4 weeks (Fig. 3B), which demonstrated a significant accumulation of p-tau (Ser<sup>262</sup>) in both soma and neuronal processes, compared with the control where p-tau was mostly in the neuronal processes (Fig. 3B).

#### 3.1.3. Long-term influence of 2 min of ischaemia on PKA

To study the possible involvement of PKA in phosphorylating tau at Ser<sup>262</sup> in the 4 weeks recovery after 2 min ischaemia experiment, the level of phosphorylated CREB (p-CREB) was assessed as



**Fig. 2.** Protein assay of LKB1/AMPK axis: phosphorylated (Active) form of LKB1 (A) and AMPK (B) and the total protein of each (A, B) were analysed via Western blot of the cortical and hippocampus regions of the control, ischaemic only and ischaemia followed by short-term 60 min and long-term recovery of 4 weeks following 2 min CA ( $n = 6$  each). I-2m: 2 min ischaemia, I-2m/R- 60 m: 2 min ischaemia followed by 60 min reperfusion, I-2m/R- 4w: 2 min ischaemia followed by 4 weeks recovery period (One Way ANOVA,  $*p < 0.05$  for p-LKB1 in I-2m vs control,  $*p < 0.01$ , for p-LKB1 in I-2m/R- 4w vs control;  $*p < 0.01$ , for p-AMPK in I-2m, I-2m/R- 60 m and I-2m/R- 4w vs control). Error bars depict the SD. All values are expressed as percent change relative to control group and were corrected by the Actin level. C) Phosphorylated AMPK (green) presence in control (Fig. 2C a, b, c) and long-term recovery of 4 weeks (Fig. 2C d, e, f) are visualised by immunofluorescent staining. D) DAPI (blue) shows nuclei staining for all cell types (both neurons and glial cells). Distribution of p-AMPK within the neurons and glial cells are shown by immunofluorescent co-staining with neuronal marker for nuclei (NeuN (a), red) or cytoplasmic glial fibrillary acidic protein (GFAP (b), red) from the brain samples of long-term recovery group (2 min ischaemia followed by 4 weeks). Accumulation of p-LKB1 is shown via DAB staining in long-term recovery group (d) compared with control group (c). (For interpretation of the references to colour in this figure legend, the reader is referred to the web version of this article.)



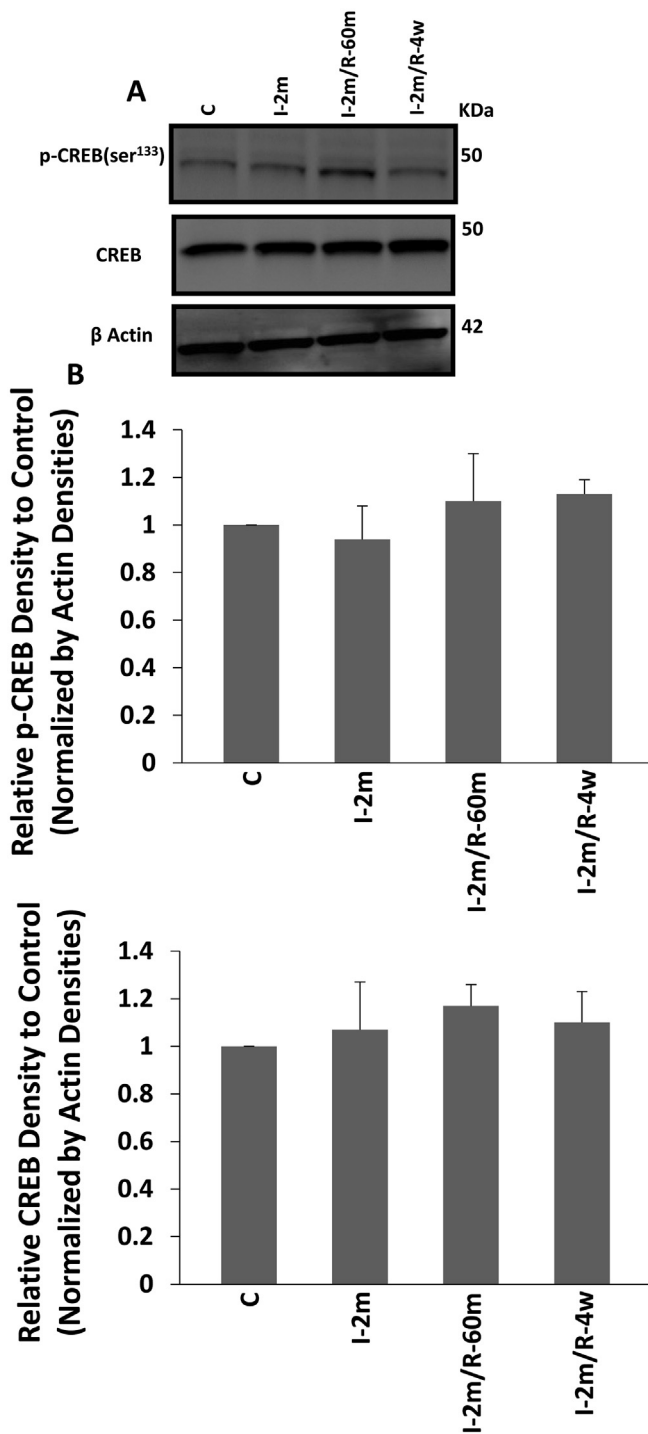


**Fig. 4.** PKA activity assessment: activation of PKA was evaluated by assessing the level of p-CREB (Ser<sup>133</sup>) and the total CREB. A) Western blot result from the brain samples of; control group, 2 min ischaemia, and 2 min ischaemia followed by 60 min and 4 weeks recovery ( $n = 6$  each). B) Analysis of the results of the western blot from the hippocampus and cortex of the same animals were done to test the levels of p-CREB and CREB. All the groups showed the same level of active CREB, an indicator of PKA activity. The same level of total CREB was seen across the experimental groups. All values are expressed as percent change relative to control group and were corrected by the Actin level. I-2m: 2 min ischaemia, I-2m/R- 60 m: 2 min ischaemia followed by 60 min reperfusion, I-2m/R- 4w: 2 min ischaemia followed by 4 weeks recovery period. Error bars depict the SD.

an indicator of PKA activity. No significant change in the level of p-CREB was observed between the control, 2 min ischaemia and 2 min ischaemia followed by 4 weeks recovery groups (One Way ANOVA) (Fig. 4), indicating that a short episode of ischaemia was not affecting PKA, during 2 min CA and after 4 weeks recovery.

### 3.1.4. Long-term influence of 2 min of ischaemia on GSK-3 $\beta$ and PP2A activities

As GSK-3 $\beta$  activity is controlled by inhibition through its Ser<sup>9</sup> phosphorylation, the level of p-GSK-3 $\beta$  (Ser<sup>9</sup>) and total GSK-3 $\beta$  were examined, after long-term recovery from 2 min CA. The results demonstrated the same level of p-GSK-3 $\beta$  (Ser<sup>9</sup>), indicating unaffected activity of GSK-3 $\beta$  by ischaemia in our model (Fig. 5A). The same levels of p-PP2A at Tyr<sup>307</sup> (inactive form) and PP2A (active form) were also observed in all groups (One Way ANOVA) (Fig. 5B). This data demonstrates that 2 min of ischaemia did not affect the activity of PP2A during ischaemia, reperfusion or long-term recovery. IF staining showed the presence of p-GSK-3 $\beta$  (Ser<sup>9</sup>), with co-localization with tau in some areas (Fig. 5C), its distribution is not obviously increased by a short episode of ischaemia in long-term recovery groups.

### 3.1.5. Effect of 2 min ischaemia on memory and learning after 4 weeks recovery

To study the effect of a short episode of 2 min brain ischaemia on learning and spatial memory, these two criteria of cognitive behaviour were assessed using the NOR and MWM. Object recognition performance was tested 1 h (Fig. 6a, b) and 24 h (Fig. 6c, d) after training with identical objects. The results showed that the animals' learning and memory (Student paired  $t$ -test) had not been reduced after 2 min CA. The mean latency finding the platform in the MWM test, indicating that spatial learning and memory in the MWM were not significantly different before, and 4 weeks after CA tests (Student paired  $t$ -test) (Fig. 6e, f). These results indicate that the hyperphosphorylation of tau at Ser<sup>262</sup> in response to ischaemia after 4 weeks recovery was not associated with detectable changes in learning and memory function in this study.

## 3.2. Human studies in AD and normal brains

To investigate whether the changes seen in response to ischaemia in animal studies were present in the brains of patients with AD, control human brains were compared with those from patients with diagnosed AD on clinical diagnosis and confirmed histologically and the following results were observed:

### 3.2.1. Tau phosphorylation at AMPK-sensitive (Ser<sup>262</sup>) and GSK-3 $\beta$ -sensitive (AT8) epitopes in hippocampus

To study the possible involvement of AMPK and GSK-3 $\beta$  as a potential mechanism behind tau phosphorylation in AD, we investigated the co-elevation of p-tau in two specific-responsive sites to two different kinases in the same samples of clinically diagnosed AD brains and normal controls. The level of p-tau (Ser<sup>262</sup>) and p-tau (Ser<sup>202</sup>/Thr<sup>205</sup> (AT8)) was significantly increased in the hippocampus of AD brains (Student  $t$ -test,  $F_{1,7} = \text{Infinity}$ ,  $*p < 0.05$ ), while the total tau protein decreased (Student  $t$ -test,  $F_{1,7} = \text{Infinity}$ ,  $*p < 0.0001$ ). The actin loading was shown across the different groups (Fig. 7).

### 3.2.2. AMPK, GSK-3 $\beta$ and PP2A activities in hippocampus of AD brains

To examine the levels of all three main enzymes in p-tau elevation in AD, the levels of p-AMPK (Thr<sup>172</sup>), p-GSK-3 $\beta$  (Ser<sup>9</sup>) and PP2A were evaluated, along with the total amount of each enzyme. A significant increase in p-AMPK (Thr<sup>172</sup>) was seen in AD brains (Student  $t$ -test,  $F_{1,7} = \text{Infinity}$ ,  $*p < 0.05$ ), while the level of the inactive

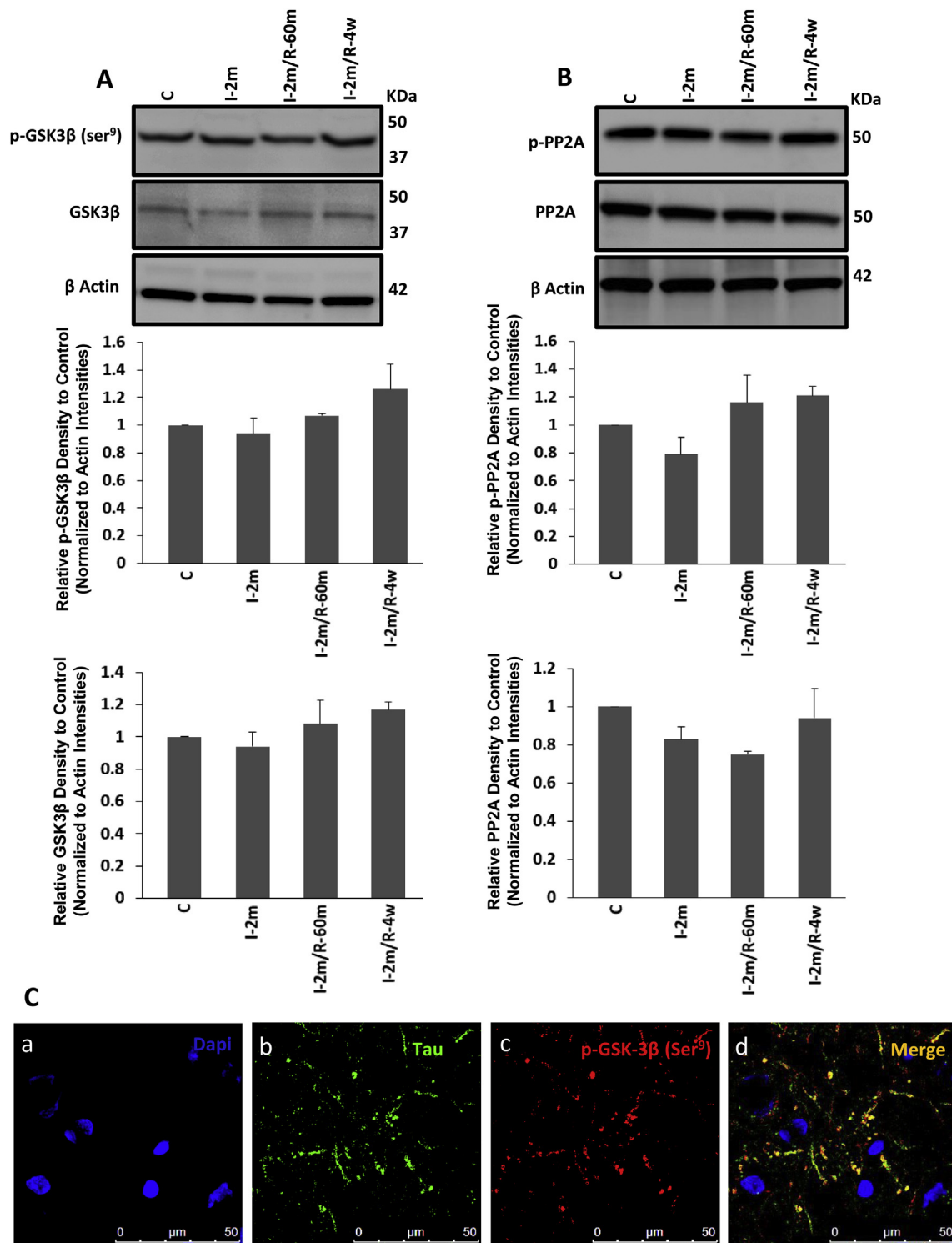


**Fig. 5.** Evaluating the activities of GSK-3 $\beta$  and PP2A: A) Western blot analyzing of the level of p-GSK-3 $\beta$  at Ser<sup>9</sup> and total protein of GSK-3 $\beta$  assessment from control group, 2 min ischaemia, and 2 min ischaemia followed by 60 min and 4 weeks recovery ( $n = 6$  each), where no significant changes were observed. B) Western blot analysis of the hippocampus and cortex of the same animals was performed to examine the levels of PP2A and p-PP2A. All the groups showed the same level of PP2A. All values are expressed as percent change relative to control group and were corrected by the Actin level. I-2m: 2 min ischaemia, I-2m/R- 60 m: 2 min ischaemia followed by 60 min reperfusion, I-2m/R- 4w: 2 min ischaemia followed by 4 weeks recovery period. (Error bars depict the SD. C) Immunofluorescent results showed the presence of p-GSK-3 $\beta$  at Ser<sup>9</sup> (inactive form; red) with some co-localization with tau protein (green) in the brain sections of the long-term groups of 4 weeks recovery following 2 min cardiac arrest (CA) contained the hippocampus and parietal cortex. DAPI (blue) shows nuclei staining for all cell types (both neurons and glial cells). (For interpretation of the references to colour in this figure legend, the reader is referred to the web version of this article.)

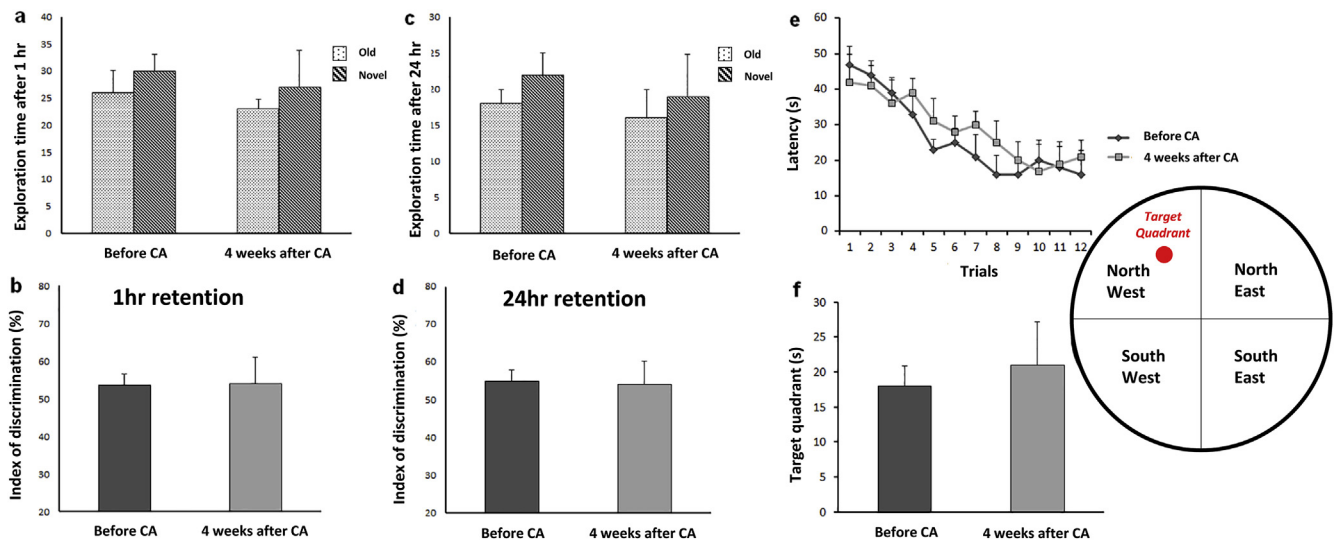


**Fig. 6.** Effects of global brain ischaemia on cognitive function after 2 min cardiac arrest (CA) ( $n = 6$ ). Learning and memory performance were evaluated in novel object recognition (NOR) (a–d) and Morris water maze (MWM) (e–f) tasks before and 4 weeks after CA ( $n = 6$ ). Performance on object recognition was tested 1 h (a–b) and 24 h (c–d) after training with two identical objects. In MWM task, spatial acquisition trial (escape latency (e) and time in target quadrant (f)) were performed in order to detect spatial learning and memory ability. Student Paired *t*-test, Data are expressed as mean  $\pm$  SD.

form of GSK-3 $\beta$ , p-GSK-3 $\beta$  (Ser<sup>9</sup>), was decreased (Student *t*-test,  $F_{1,7} = \text{Infinity}$ ,  $*p < 0.001$ ). The PP2A level also showed a significant decline (Student *t*-test,  $F_{1,7} = \text{Infinity}$ ,  $*p < 0.005$ ) in AD brains compared with the normal groups. There were no significant observed changes in the total proteins levels of AMPK and GSK-3 $\beta$ . The actin loading was shown across the different groups (Fig. 8).

#### 4. Discussion

We investigated site-specific hyperphosphorylation of tau at Ser<sup>262</sup> and at AT8 (Ser<sup>202</sup>/Thr<sup>205</sup>) by AMPK and GSK-3 $\beta$ , following brain ischaemia and its impact on the learning and memory of rats. Tau pathology in AD has been documented (Majd et al., 2015; Murray et al., 2015) and the presence of aggregated p-tau following brain hypoxia, suggests a link between hypoxia, ischaemia, AD pathological hallmarks and cognitive deficits (Madureira et al., 2001; Chen et al., 2003; Iliff et al., 2014; Zhang et al., 2014). Using a reversible model of brain ischaemia in adult female rats, Wen et al. showed an extensive neuronal tauopathy following the ischaemic insult, suggesting pathological evidence of developing AD in post-ischaemic brains (Wen et al., 2004, 2007), however it is not clear how specific ischaemia induced tau-hyperphosphorylation affects cognition. We reported an early pattern of tau dephosphorylation (Ser<sup>262</sup>), after 2 min of CA, which was consistent with previous reports of tau dephosphorylation in a transient ischaemic model of stroke and cardiac arrest (Shackelford and Yeh, 1998; Majd et al., 2016). Our data showed no re-phosphorylation following an hour of reperfusion. Here, we observed significant tau hyperphosphorylation at Ser<sup>262</sup>, a sensitive epitope to AMPK (Thornton et al., 2011; Yoshida and Goedert, 2012) occurring 4 weeks post a 2 min CA. The level of p-tau at AT8 (Ser<sup>202</sup>/Thr<sup>205</sup>), a GSK-3 $\beta$  and PKA sensitive but AMPK kinases insensitive residue (Hashiguchi et al., 2002; Liu et al., 2006; Takashima, 2006; Hanger et al., 2009; Hernandez et al., 2013) did not show any significant change during ischaemia, or recovery. Tau phosphorylation is a known indicator of altered neuronal metabolism (van der Harg et al., 2014), our results suggested the presence of a metabolic related mechanism altering p-tau status in response to alterations in neuronal oxygen supply.

The LKB1/AMPK axis has a key role as the master controller of cellular energy balance, in modulating metabolism which is

triggered by hypoxia/anoxia (Hardie, 2011). After being activated by LKB1, AMPK kinases stimulate catabolic and inhibit anabolic processes allowing the cells to adapt to hypoxia by adjusting intracellular ATP (Ramamurthy and Ronnett, 2006). It is reported that blocking the AMPK pathway, reduced tau phosphorylation in a tau mouse model of AD, showing a link between activation of the main cellular responsive kinase to ischaemia and generating p-tau, one of the main hallmarks of AD (Koppel et al., 2016).

Tau phosphorylation has been suggested as one of the main functions of the AMPK family of kinases (Thornton et al., 2011; Gu et al., 2013), which exhibit their main kinase activity on Ser<sup>262</sup>. This site is not sensitive to GSK-3 $\beta$  activity, but mainly to AMPK kinase activation as well as PKA to a lesser extent (Iijima et al., 2010; Mietelska-Porowska et al., 2014). Hyperphosphorylated tau at Ser<sup>262</sup> has been shown to be neurotoxic due to its reduced ability to bind to microtubules (Whiteman et al., 2009). We showed a significantly high level of AMPK phosphorylation, along with tau hyperphosphorylation at Ser<sup>262</sup> following 4 weeks recovery after brain ischaemia. Despite our expectation that this hyperphosphorylation might be linked to cognitive deficits, this Ser<sup>262</sup> hyperphosphorylation did not affect memory function in the animals as tested in this study. Our findings from human AD brains revealed the hyperphosphorylation of tau at multiple sites of Ser<sup>262</sup>, Ser<sup>202</sup> and Thr<sup>205</sup>. We also showed that AD brains contained a higher level of p-AMPK, an enhanced level of p-GSK-3 $\beta$  at Ser<sup>9</sup> and lower levels of PP2A at the same time, while our observations from animal models of global brain ischaemia, showed no obvious change in tau phosphorylation at its GSK-3 $\beta$ -sensitive epitopes of Ser<sup>202</sup>/Thr<sup>205</sup>, indicating the same total GSK-3 $\beta$  activity during ischaemia and after long-term recovery. Phosphorylated GSK-3 $\beta$ , PP2A and PKA along with their total levels also remained almost constant across all groups. These findings suggest that tau phosphorylation in response to a short term ischaemia is linked to AMPK kinases rather than GSK-3 $\beta$ , PP2A or PKA, and raised the possibility of requirement of a combination of tau kinase/phosphatase activity involving multiple phosphorylation sites in order to affect memory function.

Our ischaemic model provided the opportunity to separate the effects of tau phosphorylation (Ser<sup>262</sup>) from phosphorylation at Ser<sup>202</sup>/Thr<sup>205</sup>. An *in vitro* study showed that tau phosphorylated at Ser<sup>262</sup> decreased the tau assembly into paired helical filaments

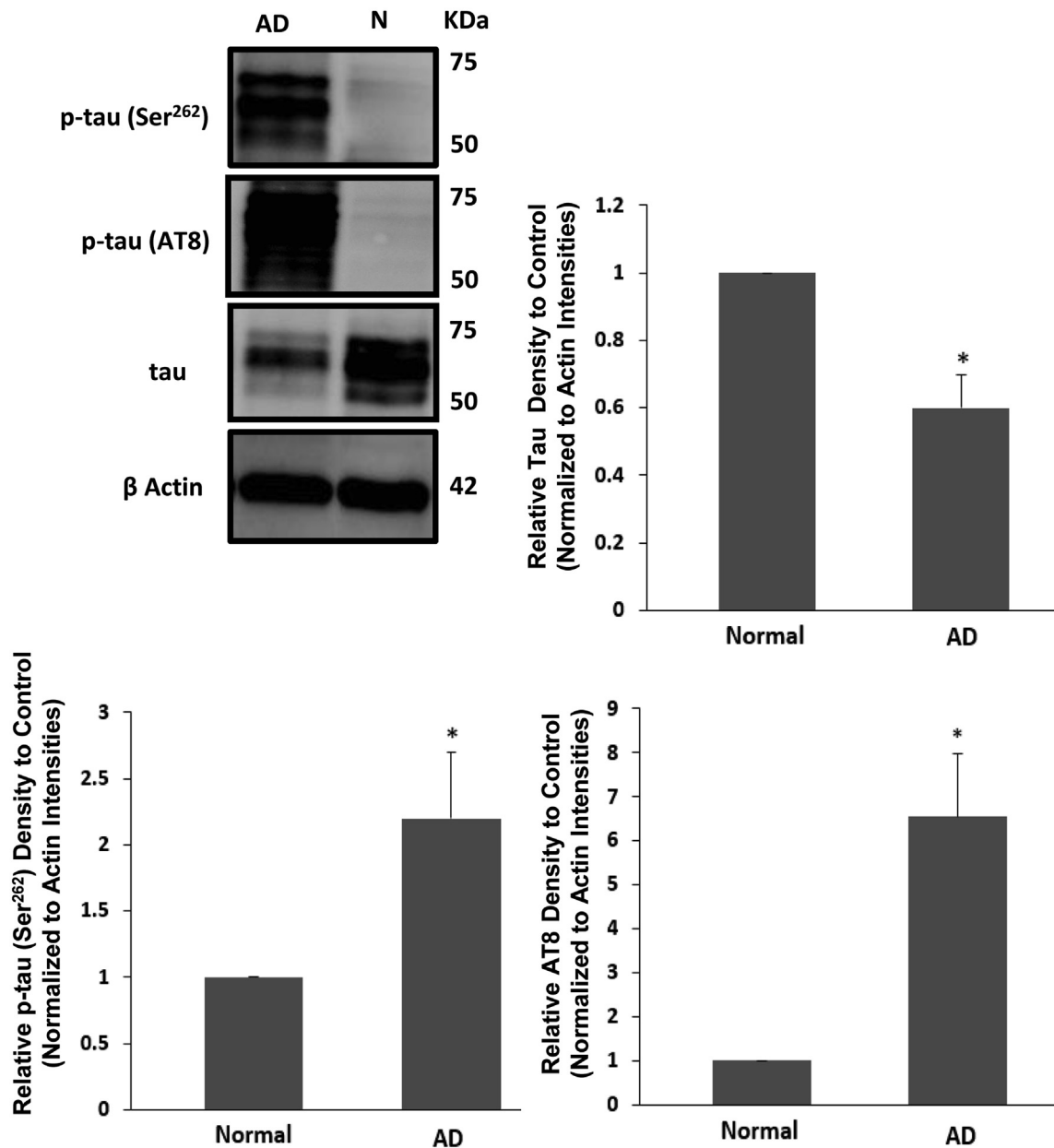


**Fig. 7.** Tau phosphorylation assessment in two specific residues of Ser<sup>262</sup> and Ser<sup>202</sup>/Thr<sup>205</sup> (AT8) from the human brains of Alzheimer's disease (AD) (n = 6) and normal groups (n = 3) (N): western blot analysis p-tau (Ser<sup>262</sup> and Ser<sup>202</sup>/Thr<sup>205</sup> (AT8)) showed the elevation of both forms of p-tau in the AD brains compared with normal groups brains (Student t-test, \**p* < 0.05). Total tau protein was also tested via western blot of the same brain samples from the hippocampus and mid-frontal gyrus (MFG) of the same patients, showing a decrease in the total tau expression (Student t-test, \**p* < 0.0001). The actin loading has been showed across the different groups. Error bars depict the SD. All values are expressed as percent change relative to control group and were corrected by the Actin level.

(Schneider et al., 1999). Our data revealed that hyperphosphorylation of Ser<sup>262</sup> alone after ischaemia was not associated with memory and learning impairment in this study. Previous studies have reported that hyperphosphorylated tau is involved in dysfunctional axonal transport with evidence of a toxic effect of tau phosphorylated at (Ser<sup>262</sup>), especially in the presence of beta amyloid (Chatterjee et al., 2009; Iijima et al., 2010). In our study, we found extensive phosphorylation of tau at both Ser<sup>262</sup> and AT8 residues in human AD brains, associated with elevation of AMPK and GSK-3 $\beta$ , however our animal model, exposed to ischaemia only showed Ser<sup>262</sup> hyperphosphorylation, unchanged AT8, and unchanged GSK3B, PP2A, PKA phosphorylated and total levels along with unaffected memory function in rats. We propose that tau hyperphosphorylation at Ser<sup>262</sup> occurred mainly due to AMPK pathway activation, as we showed that PKA levels, the other kinase

with potential tau kinase activity at Ser<sup>262</sup> (Mietelska-Porowska et al., 2014), remained unchanged. AMPK has been suggested to be a protective metabolic mechanism allowing neurons to compensate for prior ischaemic damage (Russell et al., 2004), and some reports have shown that its activation inactivates GSK-3 $\beta$  through phosphorylation of Ser<sup>9</sup> (Horike et al., 2008). Some studies, however have suggested that hypoxia directly activates GSK-3 $\beta$  (Roh et al., 2005). Observing no adverse impact following a short episode of ischaemia on memory and learning in our study, we hypothesize that ischaemic-derived activation of AMPK protects the cell by returning the ischaemic-derived GSK-3 $\beta$  hyperactivity to a normal level, with a possible protective effect against tau aggregation through the modulating effect of p-AMPK on GSK-3 $\beta$ . It is also hypothesized that Ser<sup>262</sup> phosphorylation under ischaemic situations acts as an initial trigger, enhancing the phosphoryla-

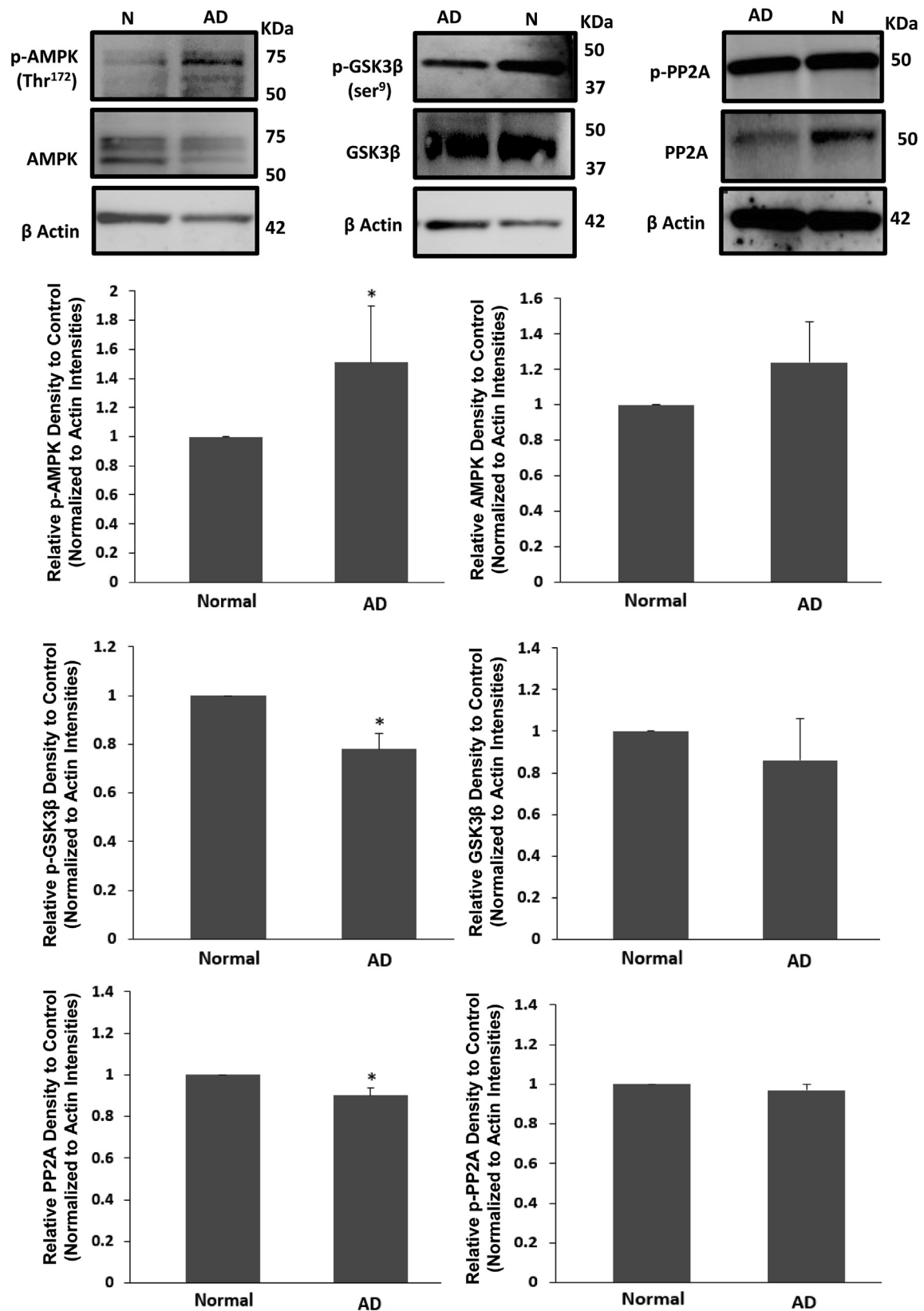


**Fig. 8.** AMPK, GSK-3β and PP2A assessment: phosphorylated forms of AMPK, GSK-3β (Ser<sup>9</sup>) and PP2A (Tyr<sup>307</sup>) along with the un-phosphorylated forms were examined via western blot analysing in the human brain samples (hippocampus and mid-frontal gurus) of Alzheimer's disease (AD) (n = 6) and normal groups (N) (n = 3). Phosphorylated AMPK (Thr<sup>172</sup>) was increased in AD brains compared with the normal groups (Student t-test, \* $p < 0.05$ ). The levels of p-GSK-3β at Ser<sup>9</sup> (inactive form) and PP2A (active form) were decreased (\* $p < 0.001$  and \* $p < 0.005$ , respectively) in AD cases where the total level of AMPK, GSK-3β and p-PP2A (inactive form) did not show any significant changes. The actin loading has been showed across the different groups. Error bars depict the SD. All values are expressed as percent change relative to control group and were corrected by the Actin level.

tion of tau over longer periods of time (up to 20 years) (Amieva et al., 2014) taken for a patient to develop the symptoms of AD. Recent research using tau toxicity models, demonstrated that phosphorylation at Ser<sup>262</sup> promoted further phosphorylation at the possible GSK3 $\beta$ -phosphorylated epitopes of AT8 (Bertrand et al., 2010). The significantly higher level of p-AMPK in the hippocampus and MFG of AD patients in our study was consistent with former reports (Thornton et al., 2011; Vingtdoux et al., 2011), providing more evidence for multifactorial-based mechanism for AD pathogenesis, however if the progressive neurodegenerative features of the disease could be a direct involvement of an individual kinase/phosphatase or the combination of them, is a question that requires further investigations. Our findings demonstrated a substantial decrease in p-GSK-3 $\beta$  at Ser<sup>9</sup> (inactive form), along with reduced activity of PP2A in the AD affected brains. Considering our results from animal and human studies and the results of previous studies (Lovell et al., 2004; Liu et al., 2005; Vingtdoux et al., 2011), we suggest that AMPK triggers a change in tau phosphorylation status following an alteration in cellular energy, initially modulating the GSK-3 $\beta$  activity, then triggering further tau phosphorylation over a longer period of time. Although the hypothesis that changes in AMPK activity and tau phosphorylation at Ser<sup>262</sup> is placed upstream of further tau phosphorylation by the other kinases (including GSK-3 $\beta$ ) still remains to be substantiated, we suggest that memory impairment is not a consequence of Ser<sup>262</sup> tau hyperphosphorylation alone and the involvement of GSK-3 $\beta$ , sometimes associated with PP2A remains a requirement for the creation of cognitive deficits, as seen in AD patients.

## 5. Conclusions

This study demonstrated the activation of the LKB1/AMPK axis secondary to ischaemia leading to hyperphosphorylation of tau at the AMPK-sensitive epitope (Ser<sup>262</sup>) after 4 weeks with no involvement of GSK-3 $\beta$  or PP2A and no cognition/memory deficits, while our AD brain study showed elevated p-AMPK (Thr<sup>172</sup>) and p-GSK-3 $\beta$  (Ser<sup>9</sup>) and reduced PP2A levels. We propose that AMPK begins the process of tau phosphorylation in response to ischaemia with a possible modulating influence on GSK-3 $\beta$  initially however phosphorylation at Ser<sup>262</sup> may facilitate tau phosphorylation in other residues, in situations of prolonged hypoxia. We suggest that a GSK-3 $\beta$  and/or PP2A presence is required to produce memory impairment associated with metabolic disturbances in the brain environment. The specific impact of the early activated AMPK pathway on the other tau kinases and the level of involvement of different AMPK kinases in generating the observed phenomenon responsible for tau hyperphosphorylation in response to hypoxia remained to be evaluated in our future studies, particularly if the hypoxic insult persists or is repeated.

## Conflict of interests

There are no conflicts of interest to disclose in this study.

## Acknowledgements

This study was supported by the project grant from the Australian Resuscitation Council (RPF13/771) and Flinders University Establishment grant (39468). The authors would like to thank the Flinders Biomedical Engineering Department, Mark McEwen and Noel Kitto for technical support, the Animal and Microscopy Facilities of Flinders University, Dr. Timothy Chataway, and the Alzheimer's and Parkinson diseases' lab especially Fariba Chegini for their enthusiastic discussions and support. We also acknowl-

edge Ms Robyn Flook and the South Australian Brain Bank in supplying all the brain tissue used in this study.

All authors were involved in the study design and development of the model. SM and HG were responsible for completing the experiments. The initial draft was written by SM and reviewed by HG and JP.

## References

- Amieva, H., Mokri, H., Le Goff, M., Meillon, C., Jacqmin-Gadda, H., Foubert-Samier, A., Orgogozo, J.M., Stern, Y., Dartigues, J.F., 2014. Compensatory mechanisms in higher-educated subjects with Alzheimer's disease: a study of 20 years of cognitive decline. *Brain* 137, 1167–1175.
- Asai, H., Ikezu, S., Tsunoda, S., Medalla, M., Luebke, J., Haydar, T., Wolozin, B., Butovsky, O., Kugler, S., Ikezu, T., 2015. Depletion of microglia and inhibition of exosome synthesis halt tau propagation. *Nat. Neurosci.* 18, 1584–1593.
- Augustinack, J.C., Schneider, A., Mandelkow, E.M., Hyman, B.T., 2002. Specific tau phosphorylation sites correlate with severity of neuronal cytopathology in Alzheimer's disease. *Acta neuropathol.* 103, 26–35.
- Bertrand, J., Plouffe, V., Senechal, P., Leclerc, N., 2010. The pattern of human tau phosphorylation is the result of priming and feedback events in primary hippocampal neurons. *Neuroscience* 168, 323–334.
- Bevins, R.A., Besheer, J., 2006. Object recognition in rats and mice: a one-trial non-matching-to-sample learning task to study 'recognition memory'. *Nat. Protoc.* 1, 1306–1311.
- Castro-Alvarez, J.F., Gutierrez-Vargas, J., Darnaudery, M., Cardona-Gomez, G.P., 2011. ROCK inhibition prevents tau hyperphosphorylation and p25/CDK5 increase after global cerebral ischemia. *Behav. Neurosci.* 125, 465–472.
- Chatterjee, S., Sang, T.K., Lawless, G.M., Jackson, G.R., 2009. Dissociation of tau toxicity and phosphorylation: role of GSK-3 $\beta$ , MARK and Cdk5 in a *Drosophila* model. *Hum. Mol. Genet.* 18, 164–177.
- Chen, G.J., Xu, J., Lahousse, S.A., Caggiano, N.L., de la Monte, S.M., 2003. Transient hypoxia causes Alzheimer-type molecular and biochemical abnormalities in cortical neurons: potential strategies for neuroprotection. *J. Alzheimer's Dis.* 16, 209–228.
- Dewar, D., Dawson, D., 1995. Tau protein is altered by focal cerebral ischaemia in the rat: an immunohistochemical and immunoblotting study. *Brain Res.* 684, 70–78.
- Domise, M., Didier, S., Marinangeli, C., Zhao, H., Chandakkar, P., Buee, L., Viollet, B., Davies, P., Marambaud, P., Vingtdoux, V., 2016. AMP-activated protein kinase modulates tau phosphorylation and tau pathology in vivo. *Sci. Rep.* 6, 26758.
- Eldar-Finkelman, H., 2002. Glycogen synthase kinase 3: an emerging therapeutic target. *Trends Mol. Med.* 8, 126–132.
- Gong, C.X., Shaikh, S., Wang, J.Z., Zaidi, T., Grundke-Iqbal, I., Iqbal, K., 1995. Phosphatase activity toward abnormally phosphorylated tau: decrease in Alzheimer disease brain. *J. Neurochem.* 65, 732–738.
- Gu, G.J., Wu, D., Lund, H., Sunnemark, D., Kvist, A.J., Milner, R., Eckersley, S., Nilsson, L.N., Agerman, K., Landegren, U., Kamali-Moghaddam, M., 2013. Elevated MARK2-dependent phosphorylation of Tau in Alzheimer's disease. *J. Alzheimer's Dis.* 33, 699–713.
- Guerra-Araiza, C., Amorim, M.A., Camacho-Arroyo, I., Garcia-Segura, L.M., 2007. Effects of progesterone and its reduced metabolites, dihydroprogesterone and tetrahydroprogesterone, on the expression and phosphorylation of glycogen synthase kinase-3 and the microtubule-associated protein tau in the rat cerebellum. *Dev. Neurobiol.* 67, 510–520.
- Hanger, D.P., Anderton, B.H., Noble, W., 2009. Tau phosphorylation: the therapeutic challenge for neurodegenerative disease. *Trends Mol. Med.* 15, 112–119.
- Hanger, D.P., Byers, H.L., Wray, S., Leung, K.Y., Saxton, M.J., Seereeram, A., Reynolds, C.H., Ward, M.A., Anderton, B.H., 2007. Novel phosphorylation sites in tau from Alzheimer brain support a role for casein kinase 1 in disease pathogenesis. *J. Biol. Chem.* 282, 23645–23654.
- Hanger, D.P., Noble, W., 2011. Functional implications of glycogen synthase kinase-3-mediated tau phosphorylation. *Int. J. Alzheimer's Dis.* 2011, 352805.
- Hardie, D.G., 2011. AMP-activated protein kinase: a cellular energy sensor with a key role in metabolic disorders and in cancer. *Biochem. Soc. Trans.* 39, 1–13.
- Hashiguchi, M., Saito, T., Hisanaga, S., Hashiguchi, T., 2002. Truncation of CDK5 activator p35 induces intensive phosphorylation of Ser202/Thr205 of human tau. *J. Biol. Chem.* 277, 44525–44530.
- Hernandez, F., Lucas, J.J., Avila, J., 2013. GSK3 and tau: two convergence points in Alzheimer's disease. *J. Alzheimer's Dis.* 33 (Suppl. 1), S141–S144.
- Horike, N., Sakoda, H., Kushiya, A., Ono, H., Fujishiro, M., Kamata, H., Nishiyama, K., Uchijima, Y., Kurihara, Y., Kurihara, H., Asano, T., 2008. AMP-activated protein kinase activation increases phosphorylation of glycogen synthase kinase 3 $\beta$  and thereby reduces cAMP-responsive element transcriptional activity and phosphoenolpyruvate carboxylase C gene expression in the liver. *J. Biol. Chem.* 283, 33902–33910.
- Iijima, K., Gatt, A., Iijima-Ando, K., 2010. Tau Ser262 phosphorylation is critical for Abeta42-induced tau toxicity in a transgenic *Drosophila* model of Alzheimer's disease. *Hum. Mol. Genet.* 19, 2947–2957.
- Iliff, J.J., Chen, M.J., Plog, B.A., Zeppenfeld, D.M., Soltero, M., Yang, L., Singh, I., Deane, R., Nedergaard, M., 2014. Impairment of glymphatic pathway function promotes tau pathology after traumatic brain injury. *J. Neurosci.* 34, 16180–16193.

- Johnson, G.V., Stoothoff, W.H., 2004. Tau phosphorylation in neuronal cell function and dysfunction. *J. cell Sci.* 117, 5721–5729.
- Koppel, J., Jimenez, H., Adrien, L., Greenwald, B.S., Marambaud, P., Cinamon, E., Davies, P., 2016. Haloperidol inactivates AMPK and reduces tau phosphorylation in a tau mouse model of Alzheimer's disease. *Alzheimer's Disease Transl. Res. Clin. Interventions* 2, 121–130.
- Liu, F., Grundke-Iqbal, I., Iqbal, K., Gong, C.X., 2005. Contributions of protein phosphatases PP1, PP2A, PP2B and PP5 to the regulation of tau phosphorylation. *Eur. J. Neurosci.* 22, 1942–1950.
- Liu, F., Liang, Z., Shi, J., Yin, D., El-Akkad, E., Grundke-Iqbal, I., Iqbal, K., Gong, C.X., 2006. PKA modulates GSK-3 $\beta$ - and cdk5-catalyzed phosphorylation of tau in site- and kinase-specific manners. *FEBS Lett.* 580, 6269–6274.
- Lovell, M.A., Xiong, S., Xie, C., Davies, P., Markesbery, W.R., 2004. Induction of hyperphosphorylated tau in primary rat cortical neuron cultures mediated by oxidative stress and glycogen synthase kinase-3. *J. Alzheimer's Dis. JAD* 6 (659–671), 673–681, discussion.
- Madureira, S., Guerreiro, M., Ferro, J.M., 2001. Dementia and cognitive impairment three months after stroke. *Eur. J. neurology* 8, 621–627.
- Mairet-Coello, G., Courchet, J., Pieraut, S., Courchet, V., Maximov, A., Polleux, F., 2013. The CAMKK2-AMPK kinase pathway mediates the synaptotoxic effects of Abeta oligomers through Tau phosphorylation. *Neuron* 78, 94–108.
- Majd, S., Power, J.H., Grantham, H.J., 2015. Neuronal response in Alzheimer's and Parkinson's disease: the effect of toxic proteins on intracellular pathways. *BMC Neurosci.* 16, 69.
- Majd, S., Power, J.H., Koblar, S.A., Grantham, H.J., 2016 Aug. Early glycogen synthase kinase-3 $\beta$  and protein phosphatase 2A independent tau dephosphorylation during global brain ischaemia and reperfusion following cardiac arrest and the role of the adenosine monophosphate kinase pathway. *Eur. J. Neurosci.* 44 (3), 1987–1997, <http://dx.doi.org/10.1111/ejn.13277>.
- Majd SP, J.H., Koblar, S.A., Grantham, H.J.M., 2016. Introducing a developed model of reversible cardiac arrest to produce global brain ischemia and its impact on microtubule-associated protein tau phosphorylation at Ser396. *Int. Neurology Neurother.* 3, 1–6.
- Mateen, F.J., Josephs, K.A., Trenerry, M.R., Felmlee-Devine, M.D., Weaver, A.L., Carone, M., White, R.D., 2011. Long-term cognitive outcomes following out-of-hospital cardiac arrest: a population-based study. *Neurology* 77, 1438–1445.
- Mietelska-Porowska, A., Wasik, U., Goras, M., Filipek, A., Niewiadomska, G., 2014. Tau protein modifications and interactions: their role in function and dysfunction. *Int. J. Mol. Sci.* 15, 4671–4713.
- Murray, M.E., Lowe, V.J., Graff-Radford, N.R., Liesinger, A.M., Cannon, A., Przybelski, S.A., Rawal, B., Parisi, J.E., Petersen, R.C., Kantarci, K., Ross, O.A., Duara, R., Knopman, D.S., Jack Jr., C.R., Dickson, D.W., 2015. Clinicopathologic and 11C-Pittsburgh compound B implications of Thal amyloid phase across the Alzheimer's disease spectrum. *Brain a J. neurology* 138, 1370–1381.
- Plassman, B.L., Havlik, R.J., Steffens, D.C., Helms, M.J., Newman, T.N., Drosdick, D., Phillips, C., Gau, B.A., Welsh-Bohmer, K.A., Burke, J.R., Guralnik, J.M., Breitner, J.C., 2000. Documented head injury in early adulthood and risk of Alzheimer's disease and other dementias. *Neurology* 55, 1158–1166.
- Pohjasvaara, T., Erkinjuntti, T., Ylikoski, R., Hietanen, M., Vataja, R., Kaste, M., 1998. Clinical determinants of poststroke dementia. *Stroke. a J. Cereb. circulation* 29, 75–81.
- Power, J.H., Barnes, O.L., Chegini, F., 2015. Lewy Bodies and the Mechanisms of Neuronal Cell Death in Parkinson's Disease and Dementia with Lewy Bodies. *Brain pathology, Zurich, Switzerland.*
- Ramamurthy, S., Ronnett, G.V., 2006. Developing a head for energy sensing: AMP-activated protein kinase as a multifunctional metabolic sensor in the brain. *J. physiology* 574, 85–93.
- Roh, M.S., Eom, T.Y., Zmijewska, A.A., De Sarno, P., Roth, K.A., Jope, R.S., 2005. Hypoxia activates glycogen synthase kinase-3 in mouse brain in vivo: protection by mood stabilizers and imipramine. *Biol. psychiatry* 57, 278–286.
- Russell 3rd, R.R., Li, J., Coven, D.L., Pypaert, M., Zechner, C., Palmeri, M., Giordano, F.J., Mu, J., Birnbaum, M.J., Young, L.H., 2004. AMP-activated protein kinase mediates ischemic glucose uptake and prevents postischemic cardiac dysfunction, apoptosis, and injury. *J. Clin. investigation* 114, 495–503.
- Schneider, A., Biernat, J., von Bergen, M., Mandelkow, E., Mandelkow, E.M., 1999. Phosphorylation that detaches tau protein from microtubules (Ser262, Ser214) also protects it against aggregation into Alzheimer paired helical filaments. *Biochemistry* 38, 3549–3558.
- Shackelford, D.A., Yeh, R.Y., 1998. Dephosphorylation of tau during transient forebrain ischemia in the rat. *Mol. Chem. neuropathology* 34, 103–120, sponsored by the International Society for Neurochemistry and the World Federation of Neurology and research groups on neurochemistry and cerebrospinal fluid.
- Sontag, E., Luangpirom, A., Hladik, C., Mudrak, I., Ogris, E., Speciale, S., White 3rd, C.L., 2004. Altered expression levels of the protein phosphatase 2A A $\beta$  kinase enzyme are associated with Alzheimer disease pathology. *J. neuropathology Exp. neurology* 63, 287–301.
- Stephenson, D.T., Rash, K., Clemens, J.A., 1992. Amyloid precursor protein accumulates in regions of neurodegeneration following focal cerebral ischemia in the rat. *Brain Res.* 593, 128–135.
- Stoothoff, W.H., Johnson, G.V., 2005. Tau phosphorylation: physiological and pathological consequences. *Biochimica biophysica acta* 1739, 280–297.
- Sun, J.H., Tan, L., Yu, J.T., 2014. Post-stroke cognitive impairment: epidemiology, mechanisms and management. *Ann. Transl. Med.* 2, 80.
- Takashima, A., 2006. GSK-3 is essential in the pathogenesis of Alzheimer's disease. *J. Alzheimer's Dis. JAD* 9, 309–317.
- Thornton, C., Bright, N.J., Sastre, M., Muckett, P.J., Carling, D., 2011. AMP-activated protein kinase (AMPK) is a tau kinase, activated in response to amyloid beta-peptide exposure. *Biochem. J.* 434, 503–512.
- Tonkiss, J., Shultz, P.L., Bonnie, K.E., Hudson, J.L., Duran, P., Galler, J.R., 2003. Spatial learning deficits induced by muscimol and CL218,872: lack of effect of prenatal malnutrition. *Nutr. Neurosci.* 6, 379–387.
- van der Harg, J.M., Nolle, A., Zwart, R., Boerema, A.S., van Haastert, E.S., Strijkstra, A.M., Hoozemans, J.J., Scheper, W., 2014. The unfolded protein response mediates reversible tau phosphorylation induced by metabolic stress. *Cell death Dis.* 5, e1393.
- Vingtdoux, V., Davies, P., Dickson, D.W., Marambaud, P., 2011. AMPK is abnormally activated in tangle- and pre-tangle-bearing neurons in Alzheimer's disease and other tauopathies. *Acta neuropathol.* 121, 337–349.
- Wen, Y., Yang, S., Liu, R., Brun-Zinkernagel, A.M., Koulen, P., Simpkins, J.W., 2004. Transient cerebral ischemia induces aberrant neuronal cell cycle re-entry and Alzheimer's disease-like tauopathy in female rats. *J. Biol. Chem.* 279, 22684–22692.
- Wen, Y., Yang, S.H., Liu, R., Perez, E.J., Brun-Zinkernagel, A.M., Koulen, P., Simpkins, J.W., 2007. Cdk5 is involved in NFT-like tauopathy induced by transient cerebral ischemia in female rats. *Biochimica biophysica acta* 1772, 473–483.
- Whiteman, I.T., Gervasio, O.L., Cullen, K.M., Guillemin, G.J., Jeong, E.V., Witting, P.K., Antao, S.T., Minamide, L.S., Bamburg, J.R., Goldsby, C., 2009. Activated actin-depolymerizing factor/cofilin sequesters phosphorylated microtubule-associated protein during the assembly of alzheimer-like neuritic cytoskeletal striations. *J. Neurosci. official J. Soc. Neurosci.* 29, 12994–13005.
- Xie, H., Ray, P.E., Short, B.L., 2005. NF- $\kappa$ B activation plays a role in superoxide-mediated cerebral endothelial dysfunction after hypoxia/reoxygenation. *Stroke. a J. Cereb. circulation* 36, 1047–1052.
- Yoshida, H., Goedert, M., 2012. Phosphorylation of microtubule-associated protein tau by AMPK-related kinases. *J. Neurochem.* 120, 165–176.
- Zhang, C.E., Yang, X., Li, L., Sui, X., Tian, Q., Wei, W., Wang, J., Liu, G., 2014. Hypoxia-induced tau phosphorylation and memory deficit in rats. *Neuro-degenerative Dis.* 14, 107–116.